

Copyright
by
Tylan Nixon Templin
2019

**The Thesis Committee for Tylan Nixon Templin
Certifies that this is the approved version of the following Thesis:**

**The Influence of Load Carriage and Foot Stiffness on Knee Joint
Loading and Metabolic Cost during Amputee Walking**

**APPROVED BY
SUPERVISING COMMITTEE:**

Richard R. Neptune, Supervisor

Glenn K. Klute

**The Influence of Load Carriage and Foot Stiffness on Knee Joint
Loading and Metabolic Cost during Amputee Walking**

by

Tylan Nixon Templin

Thesis

Presented to the Faculty of the Graduate School of

The University of Texas at Austin

in Partial Fulfillment

of the Requirements

for the Degree of

Master of Science in Engineering

The University of Texas at Austin

May 2019

Dedication

This thesis is dedicated to my wife, Andrea Templin, and my parents Kelly and Craig Templin.

Acknowledgements

I would like to thank my advisor, Dr. Richard Neptune, for his guidance, encouragement, and feedback on my thesis and throughout my graduate career. His expertise in the field of biomechanics and mentorship has further fueled my passion for analyzing the biomechanics of human movement. I am very grateful for being welcomed into his research group and being given the opportunity to work on exciting research projects over the last two years.

Thank you to Dr. Glenn Klute at the VA Center for Limb Loss and MoBility for providing experimental data, serving on my committee, and offering feedback in the preparation of my thesis. I would also like to thank Krista Cyr for her help with the data collection and George Eli Kaufman, CPO, for prosthetic services.

Thank you to the current and past members of the Neuromuscular Biomechanics Lab for their assistance, mentorship, feedback, and friendship.

Thank you to my parents, Kelly and Craig, and brother, Ryan, for being outstanding role models for me and for their constant love and support. I also owe many thanks to my loving wife, Andrea, who is an incredible blessing to me and has been remarkably encouraging to me in all areas of my life.

This research was supported by Dept. of Veterans Affairs, Rehabilitation Research and Development Service, grants RX002974 and RX002357.

Abstract

The Influence of Load Carriage and Foot Stiffness on Knee Joint Loading and Metabolic Cost during Amputee Walking

Tylan Nixon Templin, M.S.E.

The University of Texas at Austin, 2019

Supervisor: Richard R. Neptune

Individuals experience sudden load changes during activities of daily living. This added weight places an increased demand on the muscles providing body support, forward propulsion and balance control. For non-amputees, the mechanical output from the ankle muscles are seamlessly modulated to meet the altered demands of load carriage. However, for individuals with a lower-limb amputation, the stiffness properties of standard-of-care prosthetic feet are constant and do not change with varying load conditions. Thus, lower limb amputees often develop gait asymmetries to compensate for the loss of ankle muscles, which may be exacerbated by load carriage. These asymmetries may increase the risk for developing overuse injuries and osteoarthritis in the intact knee as well as elevate the metabolic cost of walking relative to non-amputees. Unfortunately, it is not well understood how prosthetic foot stiffness and load carriage technique influences joint loading asymmetries during amputee gait. The purpose of this study was to use a forward dynamics simulation framework to assess the influence of load carriage technique and

prosthetic foot stiffness on knee joint loading and metabolic cost during amputee gait. Forward dynamics simulations were generated to track experimental amputee walking data for each loading condition (unloaded, with a backpack, and with a frontpack) and prosthetic foot condition (four commercially available elastic energy storage and return (ESAR) feet). The results of these simulations showed that amputees rely on their intact limb as a compensatory strategy to meet the increased demands of carrying a load. Carrying the load in a backpack was found to reduce metabolic cost but increase intact knee joint loading. When varying prosthetic foot stiffness, there was no consistent effect on metabolic cost or knee joint loading in any of the three loading conditions. Future work should focus on designing prosthetic components that help reduce the joint loading asymmetry and elevated metabolic cost during load carriage for lower limb amputees. In addition, the tradeoff between metabolic cost and joint loading should be considered when determining the appropriate load carriage technique.

Table of Contents

List of Figures	ix
Chapter 1: Introduction	1
Chapter 2: Methods.....	4
Musculoskeletal Model.....	4
Forward Dynamics Simulation	4
Experimental Data	6
Study Protocol.....	7
Metabolic Cost and Joint Loading	8
Chapter 3: Results	9
Joint Loading	9
Metabolic Cost.....	11
Chapter 4: Discussion	14
Joint Loading	14
Metabolic Cost.....	17
Chapter 5: Conclusion.....	21
Appendix.....	22
References	31
Vita.....	36

List of Figures

Figure 1:	Mean stance phase intact knee contact impulses (N*s) \pm one standard deviation while wearing the four study prostheses across the three loading conditions.....	9
Figure 2:	Mean stance phase residual knee contact impulses (N*s) \pm one standard deviation while wearing the four study prostheses in the three loading conditions.....	10
Figure 3:	Mean \pm one standard deviation of total average metabolic cost while wearing the four study prostheses during the three loading conditions.....	11
Figure 4:	Mean \pm one standard deviation of total average metabolic cost of intact leg muscles throughout gait cycle while wearing the SOC foot during the three loading conditions.....	12
Figure 5:	Mean \pm one standard deviation of total average metabolic cost of residual leg muscles throughout gait cycle while wearing the SOC foot in the three loading conditions.....	13
Figure 6:	A) Intact VAS muscle activity, B) mean intact VAS contribution to body support over the stance phase for each of the three loading conditions using the SOC foot, C) Mean intact leg VAS contributions to sagittal plane external moment about the center-of-mass of the body during the three loading conditions using the SOC foot. The moment was calculated by cross multiplying the distance between the foot center-of-pressure and body center-of-mass with VAS contributions to the ground reaction forces. Positive values indicate that the muscle is generating backward angular momentum.....	16

Figure 7:	A) Intact HAM muscle activity, B) mean intact HAM contribution to body support over the stance phase for each of the three loading conditions using the SOC foot, C) Mean intact leg HAM contributions to sagittal plane external moment about the center-of-mass of the body during the three loading conditions using the SOC foot. The moment was calculated by cross multiplying the distance between the foot center-of-pressure and body center-of-mass with HAM contributions to the ground reaction forces. Positive values indicate that the muscle is generating backward angular momentum.	18
Figure A1:	Mean \pm one standard deviation of total average metabolic power (W) of intact leg muscles throughout gait cycle while wearing the SF foot in the three loading conditions.	22
Figure A2:	Mean \pm one standard deviation of total average metabolic power (W) of residual leg muscles throughout gait cycle while wearing the SF foot in the three loading conditions.	22
Figure A3:	Mean \pm one standard deviation of total average metabolic power (W) of intact leg muscles throughout gait cycle while wearing the HW foot in the three loading conditions.	23
Figure A4:	Mean \pm one standard deviation of total average metabolic power (W) of residual leg muscles throughout gait cycle while wearing the HW foot in the three loading conditions.	23
Figure A5:	Mean \pm one standard deviation of total average metabolic power (W) of intact leg muscles throughout gait cycle while wearing the DK foot in the three loading conditions.	24

Figure A6: Mean \pm one standard deviation of total average metabolic power (W) of residual leg muscles throughout gait cycle while wearing the DK foot in the three loading conditions.	24
Figure A7: Mean intact muscle forces while wearing the four study prostheses across the three loading conditions.	25
Figure A8: Mean residual muscle forces while wearing the four study prostheses across the three loading conditions.	26
Figure A9: Mean intact and residual muscle contributions to body support impulses while wearing the four study prostheses across the three loading conditions.	27
Figure A11: Mean intact leg muscle contributions to sagittal plane external moment about the center-of-mass of the body while wearing the four study prostheses across the three loading conditions.	29
Figure A12: Mean residual leg muscle contributions to sagittal plane external moment about the center-of-mass of the body while wearing the four study prostheses across the three loading conditions.	30

Chapter 1: Introduction

For individuals with lower limb amputation who are capable of locomotion, clinicians must choose from a wide range of available prosthetic feet when prescribing a prosthesis. In addition, most major prosthetic foot manufacturers offer a range of stiffnesses that are delineated in up to nine stiffness categories. Typically, clinicians prescribe prosthetic foot stiffness based on the weight and activity level of the patient. A heavier and/or more active individual would be prescribed a stiffer foot. In general, each stiffness category is intended to be used by individuals within a 10 kg range (~7% of body weight). However, the load borne by a prosthesis can change suddenly during activities of daily living such as when an individual carries a load in their arms or a backpack. If this load exceeds 10 kg, an immediate change to a prosthetic foot with increased stiffness would be recommended.

For non-amputees, the mechanical output from the ankle muscles are seamlessly modulated to meet the altered demands of load carriage (McGowan et al., 2009). However, the properties of passive prosthetic feet, such as stiffness, are constant and are not modulated with load condition. As a result, amputees respond to the increased load with greater metabolic costs (Schnall et al., 2012) and biomechanical asymmetries such as increased intact limb power generation and absorption and increased prosthetic foot dorsiflexion during late stance (Doyle et al., 2014, 2015; Schnall et al., 2014). These altered gait mechanics and asymmetries can lead to the onset of joint disorders. In particular, below-knee amputees have an increased prevalence of osteoarthritis in their intact leg

relative to their residual leg and non-amputees (Burke et al., 1978; Norvell et al., 2005; Struyf et al., 2009).

A prosthetic foot with increased stiffness would be beneficial during load carriage to avoid excessive dorsiflexion of the prosthetic foot during stance (Klodd et al., 2010), but would be undesirable during unloaded walking because the energy storage and return function which facilitates locomotion, is reduced (Fey et al., 2011). To help mitigate these undesirable outcomes, clinicians can prescribe a heel wedge or a dual keel prosthetic foot for individuals who expect to regularly carry a heavy load. The heel wedge stiffens the heel, and the dual keel prosthetic foot stiffens the keel at elevated loads when the primary keel engages the secondary keel. However, the biomechanical benefits of these prosthetic feet during various load carriage conditions remain uncertain.

Previously, musculoskeletal modeling and simulation tools have been used to analyze individual muscle and prosthetic foot-ankle contributions to body support and forward propulsion during walking (e.g., Silverman and Neptune, 2012; Zmitrewicz et al. 2007). In addition, a series of experimental and modeling studies have shown how lower limb muscles adapt to altered loading conditions (McGowan et al., 2009; McGowan et al., 2008). Collectively, these studies have highlighted the critical role of the ankle plantarflexors in contributing to the vertical ground reaction force impulse (body support), positive horizontal trunk work (forward propulsion), and modulation of mechanical output of the leg in response to increased need for body support and forward propulsion. Musculoskeletal simulations have also helped to quantify other biomechanical metrics that are difficult to analyze with experimental data alone such as knee joint loading (Sasaki and

Neptune, 2010; Shelburne et al., 2005) and metabolic cost (Umberger, 2010). Furthermore, studies have shown that joint loading and metabolic cost are influenced by changes in prosthetic foot stiffness, and that there is an optimal stiffness that minimizes these metrics during unloaded walking (Fey et al., 2012). Together, these previous simulation studies suggest that added loads may cause biomechanical gait deviations and altering the prosthesis used may reduce these gait deviations and improve walking performance.

The purpose of this study was to use a forward dynamics simulation framework to provide insight into the relationships between prosthetic foot stiffness and load carriage technique (anterior versus posterior carriage) on energy expenditure and joint loading. We expect that there is an optimal prosthetic foot that minimizes energy expenditure and joint loading for the different loading conditions. Understanding these relationships and their influence on amputee walking performance can help guide prosthetic foot prescription, and improve amputee mobility.

Chapter 2: Methods

MUSCULOSKELETAL MODEL

A transtibial musculoskeletal model was created by modifying the “gait2392” model. Briefly, the segments distal to the right tibia were replaced with a transected tibia, pylon-socket, and ankle-foot prosthesis with inertial properties adapted from LaPrè et al. (2018). The hip joint was modeled with three degrees of freedom (flexion/extension, internal/external rotation, adduction/abduction), while the knee and intact ankle were modeled as one degree of freedom pin joints. The 6 degrees of freedom between the transected tibia and pylon-socket segment were locked, and the prosthetic ankle motion was modeled as a one degree of freedom pin joint (Fey et al., 2012; Silverman and Neptune, 2012). All muscles crossing the ankle joint were removed and a coordinate actuator was added at the ankle joint to reproduce the prosthetic ankle torque. In the loading conditions, a pack was added (posteriorly or anteriorly) to the torso segment of the model with inertial properties adapted from Dembia et al. (2017). The body representing the pack was fixed to the torso.

FORWARD DYNAMICS SIMULATION

Simulations were generated for three gait cycles in each loading and prosthetic foot condition for a total of 36 simulations (3 gait cycles x 3 loading conditions x 4 prosthetic feet) using OpenSim 3.3 (Delp et al., 2007). To perform the simulations, the model was scaled based on experimentally-measured marker data. In the static pose the maximum

error between the virtual markers placed on the model and the experimental markers was 3.2 cm and the RMS marker error was 1.8 cm. Joint angles throughout each gait cycle were calculated using an inverse kinematics algorithm to minimize error between virtual and experimental markers (Delp et al., 2007). Maximum marker error during the inverse kinematics trials were less than 3 cm and the RMS error was less than 1.5 cm. A residual reduction algorithm was used to alter the joint kinematics and model inertial properties to improve the dynamic consistency between experimentally measured kinematics and kinetics (Delp et al., 2007). The suggested mass adjustments were applied to each segment and the position of the torso center-of-mass was modified to match the recommended position. After these adjustments were made, the residual reduction algorithm was performed an additional time. The weighting of the tracking parameters was fine-tuned until peak residual forces were less than 15 N, average residuals were less than 5 N and RMS error in coordinates were less than 2 degrees or less than 2 cm for rotational and translational coordinates, respectively. During the tuning process, optimal forces for residuals were kept low, while the weight of closely tracked coordinates were incrementally decreased. Computed muscle control was then used to solve for the muscle excitations that generated the amputee walking mechanics (Delp et al., 2007). Computed muscle control solved the muscle redundancy problem at each joint by minimizing muscle activations squared while also accounting for muscle activation and deactivation dynamics (Zajac, 1989).

EXPERIMENTAL DATA

The simulations tracked experimental data collected from one male transtibial amputee (age: 68 yrs, height: 176 cm, mass: 80 kg, amputated limb: right, post-amputation: 1.5 years, modified patellar tendon-bearing socket with locking pin suspension) after providing informed consent to an Institutional Review Board-approved protocol. This subject was deemed representative because of his age (Mayfield et al., 2000), and height and weight (Fryar et al., 2018). Sixty-two reflective markers were placed on the subject using a modified version of Vicon's Plug-in-Gait full-body model. The Plug-in-Gait model was modified by adding markers to the medial malleolus, medial elbow, and first and fifth metatarsal heads. Marker clusters were used to track the thigh and upper arm segments instead of wands (Cappozzo et al., 1997). The shank segments were tracked with markers placed on the fibular head and tibial tuberosity. A 12-camera Vicon motion capture system (Vicon Motion Systems, Oxford, UK) collected kinematic data as the subject walked over-ground across five force plates (AMTI, Watertown, MA) at their self-selected walking speed (SSWS). Ground reaction force and marker data were collected at 1200 HZ and 120 Hz, respectively. GRF and marker data were filtered using a 4th-order, low-pass Butterworth filter with cutoff frequencies of 20 Hz and 6 Hz, respectively. Three successful overground walking trials were collected for each condition. A successful walking trial was defined as a trial in which foot strikes occurred on separate force plates. Prior to data collection, the SSWS was determined by asking the subject to walk down a 20 m hallway while wearing his current, clinically prescribed prosthesis at his own pace. An average of three trials was used to define their SSWS.

STUDY PROTOCOL

The subject was fit with four study prostheses in random order by a certified prosthetist using standard procedures. The prostheses used in this study were:

- 1) Vari-Flex Low Profile (Össur, Aliso Viejo, CA) category 5 prosthetic foot
(standard of care, SOC)
- 2) Vari-Flex Low Profile category 5 prosthetic foot with a 6.8° heel-stiffening
wedge (HW)
- 3) Thrive dual keel (Freedom Innovations, Irvine, CA) category 5 prosthetic foot
(DK)
- 4) Vari-Flex Low Profile category 6 prosthetic foot (one category stiffer than SOC,
SF)

The participant used his clinically prescribed socket and suspension system but the pylon length was adjusted to accommodate the height of each study prosthesis. A sock and foot cover were used to blind the participant to the study prostheses. The subject wore each of these study prostheses under three different loading conditions: unloaded (no load, NL) and with a pack carried posterior (back load, BL) and anterior (front load, FL) to their torso. Weights were placed inside the pack so that the total mass was 30 lbs. (13.6 kg). The pack was padded and included straps to secure the pack to the torso (Classic; Camelbak, Tetaluma, CA). The subject was provided a minimum of 15 minutes to acclimate to each prosthesis/load combination. Rest breaks were provided as needed at the subject's request.

METABOLIC COST AND JOINT LOADING

Instantaneous metabolic power for each muscle was determined based on the metabolic model by Umberger et al. (Uchida et al., 2016; Umberger, 2010; Umberger et al., 2003). We then calculated average metabolic power by integrating the instantaneous metabolic power with respect to time and dividing by the gait cycle duration. To determine the metabolic cost, the total average metabolic power was determined by summing the contributions from the individual muscles. The axial tibio-femoral joint contact forces in both the intact and residual limbs were determined and expressed in the tibia reference frame and time integrated over the stance phase to provide the stance phase joint contact impulses. The metabolic cost and joint contact impulses were averaged over the three gait cycles for each prosthetic foot and load carriage condition.

Chapter 3: Results

JOINT LOADING

In response to the added load in BL and FL, the intact knee joint contact impulses increased relative to NL for all prosthetic feet (Figure 1). The increase in joint contact impulses was greater during BL than FL for all feet. During NL, the SOC foot had the lowest mean joint contact impulses, while during BL and FL the SF foot had the lowest mean joint contact impulses. However, the relative differences in contact impulses within each load condition across feet were small (0-7%) relative to changes between NL and BL (14-20%) and NL and FL (10-14%).

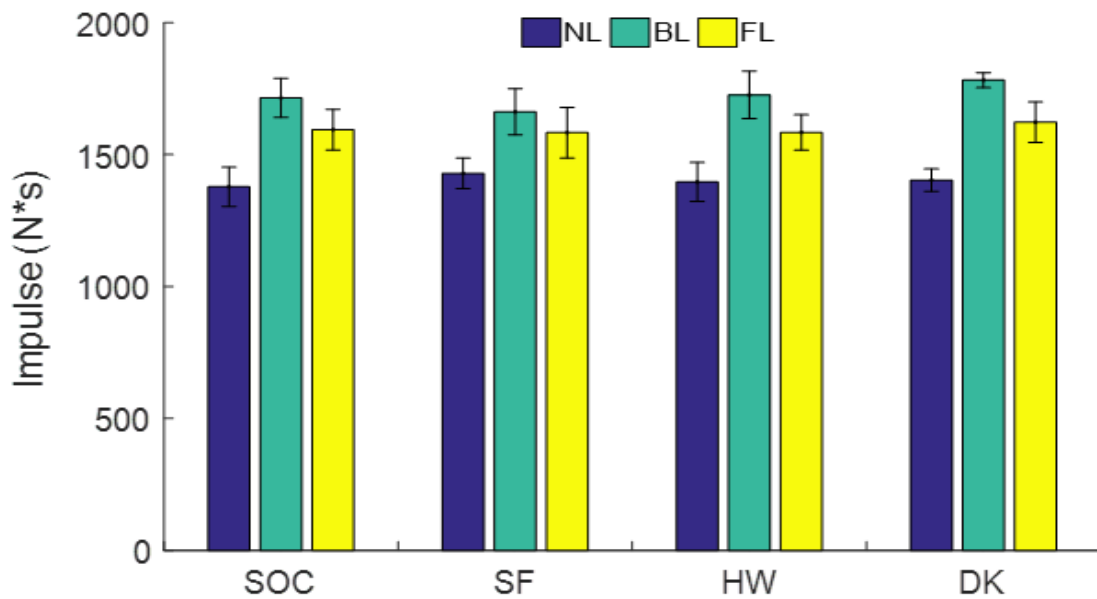


Figure 1: Mean stance phase intact knee contact impulses (N*s) \pm one standard deviation while wearing the four study prostheses across the three loading conditions.

The mean residual knee contact impulses were substantially lower than the mean intact impulses for all feet and load carriage conditions. Similar to the intact limb, the residual knee contact impulses increased during BL and FL relative to NL (Figure 2). However, the increases in residual knee contact impulse were less than the increases in the intact knee during BL and FL. Similar to the intact knee, the increase in residual contact impulse was greater during BL than FL for all feet. As with the intact knee, the relative differences in residual knee contact impulses within each load condition were small (1-9%) relative to changes between NL and BL (12-20%) and NL and FL (7-13%).

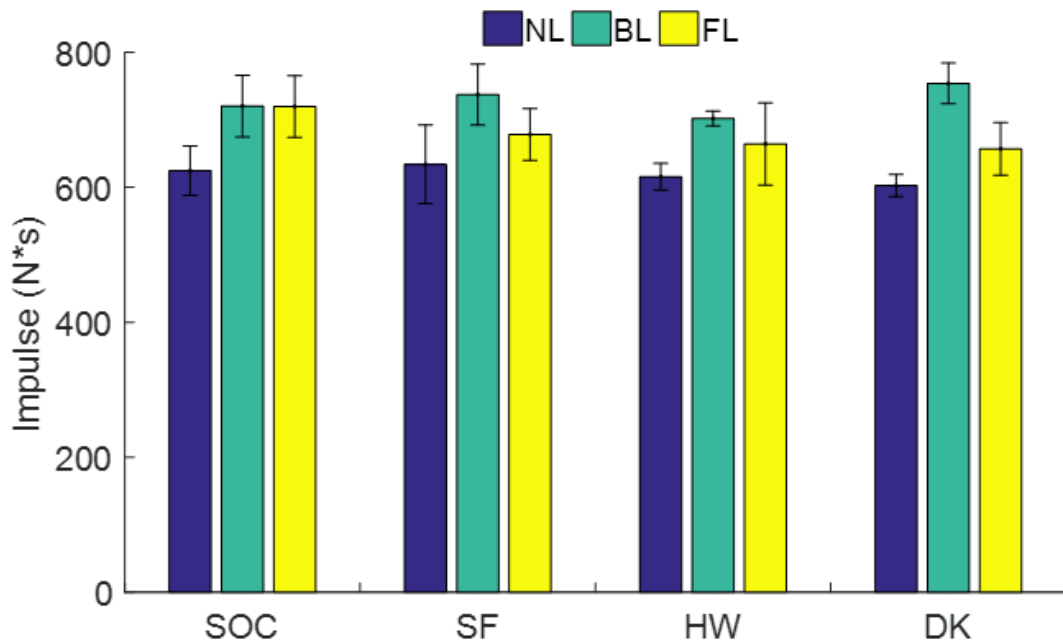


Figure 2: Mean stance phase residual knee contact impulses (N*s) \pm one standard deviation while wearing the four study prostheses in the three loading conditions.

METABOLIC COST

Both BL and FL showed increased metabolic cost relative to NL across all feet (Figure 3). However, FL consistently yielded the highest cost across feet. In NL and BL, the HW foot had the lowest cost, while in FL the SOC had the lowest cost. The relative differences in metabolic cost within each load condition were small (0-7%) relative to changes between NL and BL (7-12%) and NL and FL (11-18%).

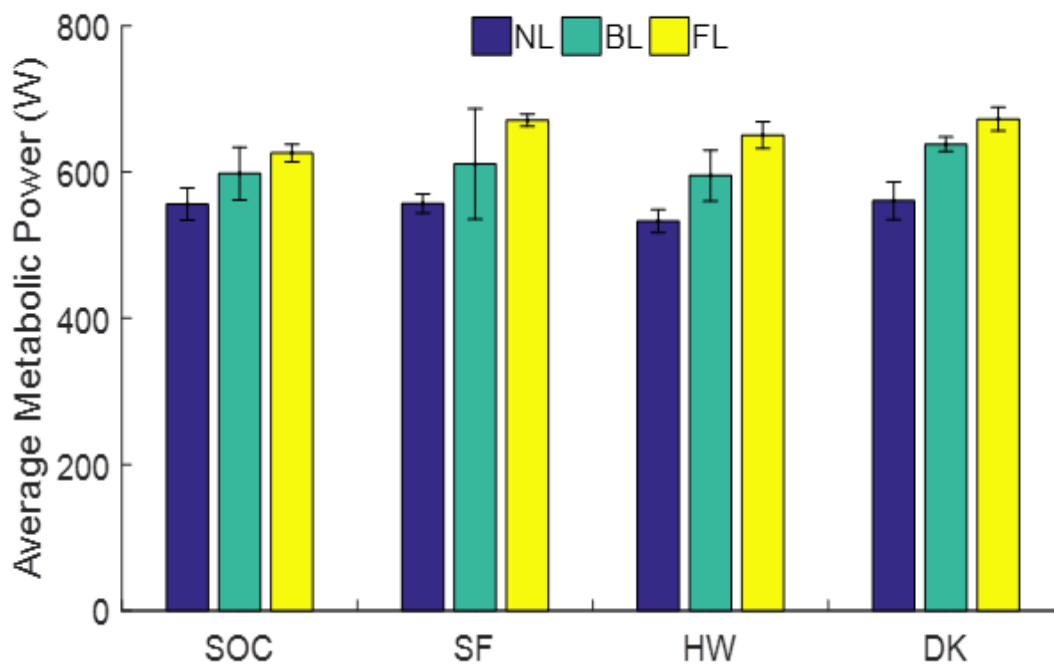


Figure 3: Mean \pm one standard deviation of total average metabolic cost while wearing the four study prostheses during the three loading conditions.

Individual muscle contributions to metabolic cost showed similar trends across feet in response to the added loads. As a result, the results below focus on the SOC foot. GAS (medial and lateral gastrocnemius), SOL (soleus), VAS (vastus medialis, vastus lateralis and vastus intermedius), and GMED (gluteus medius) showed increased cost in response to BL and FL (Figure 4). The average metabolic power consumed by SOL and GAS was greater during FL than BL. In contrast, GMED and VAS consumed more metabolic power during BL than FL. The largest change for any intact limb muscle in response to an added load was HAM (biceps femoris long head, semimembranosus, semitendinosus) during FL. GMAX (gluteus maximus), PSOAS (psoas), RF (rectus femoris), and TA (tibialis anterior) showed minimal changes in response to the loads.

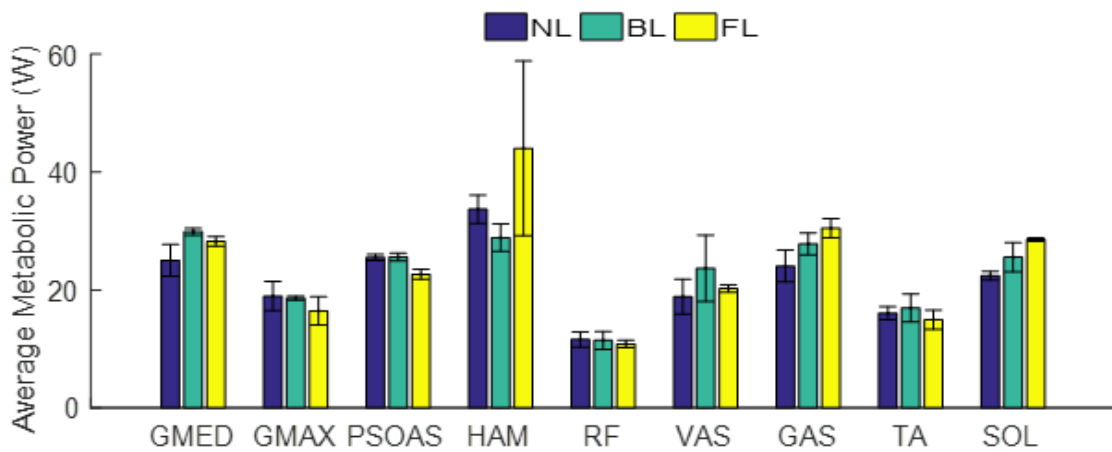


Figure 4: Mean \pm one standard deviation of total average metabolic cost of intact leg muscles throughout gait cycle while wearing the SOC foot during the three loading conditions.

In general, the residual leg muscles consumed less average metabolic power and had a lower change in metabolic cost in response to BL and FL relative to the intact leg (Figure 5). Similar to the intact limb, the residual HAM showed the greatest increase in cost during FL. GMED and GMAX showed increased cost relative to the intact limb and greater increases in response to BL and FL.

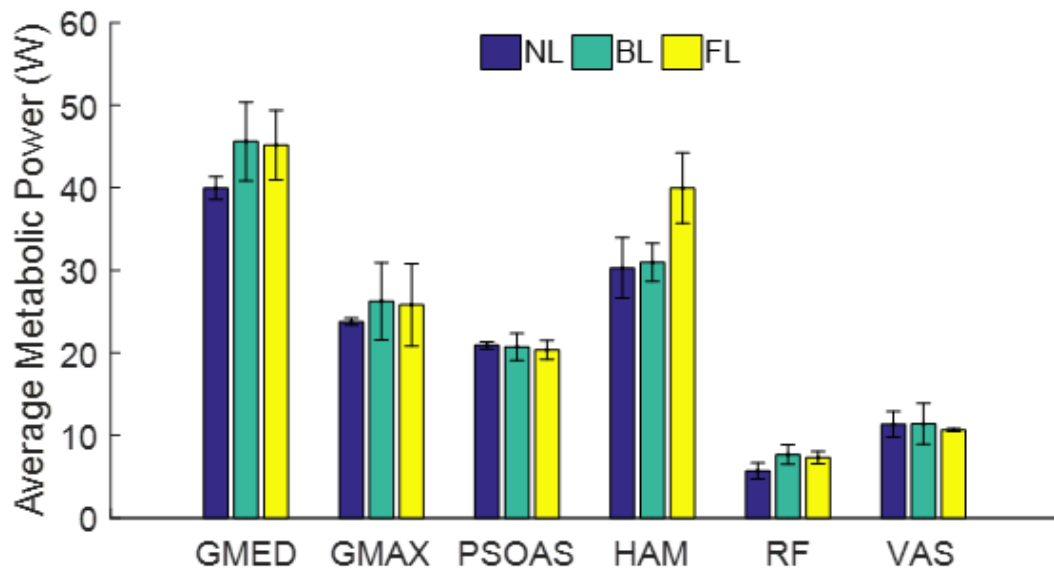


Figure 5: Mean \pm one standard deviation of total average metabolic cost of residual leg muscles throughout gait cycle while wearing the SOC foot in the three loading conditions.

Chapter 4: Discussion

The purpose of this study was to analyze the influence of load carriage technique and prosthetic foot stiffness on knee joint loading and metabolic cost for an individual with a below-knee amputation using a forward dynamics simulation framework. In response to the added loads, we found increased joint loading asymmetry and increased intact limb muscle contributions to metabolic cost relative to the residual limb. We also found a lower average metabolic cost but higher knee joint loading during BL relative to FL. In addition, we found that varying prosthetic foot stiffness did not consistently influence metabolic cost or knee joint loading in any of the three loading conditions.

JOINT LOADING

Previous studies have shown that individuals with amputation are at an increased risk of developing knee osteoarthritis in their intact limb (Burke et al., 1978; Norvell et al., 2005; Struyf et al., 2009). Our results support the expectation that the knee joint impulses experienced by the intact limb would be greater than those experienced by the residual limb in all loading conditions. In addition, we found that the imbalance between intact and residual knee loading was exacerbated in BL and FL relative to NL (Figures 1 and 2). This increased asymmetric knee loading suggests that amputees rely on their intact limb as a compensatory strategy to meet the increased demands of carrying a load. Consequently, amputees who expect to carry various loads during activities of daily living may be at an increased risk of developing knee joint disorders and ultimately osteoarthritis.

We also found that joint loading during load carriage was dependent on the location of the load, as BL resulted in greater intact and residual knee contact impulses compared to FL (Figures 1 and 2). Previously, VAS has been shown to be a primary contributor to the compressive knee contact force during unloaded walking (Silverman and Neptune, 2014) and VAS muscle activity and contributions to body support increase in response to added loads (McGowan et al., 2009). In addition, increased intact VAS muscle contributions to body support during the first half of stance has been associated with increased knee joint loading asymmetry in below-knee amputees (Fey et al., 2012). Thus, we expected VAS to exhibit increased muscle activity and contributions to body support during FL than NL and an even greater increase during BL. In addition, during BL the added posterior mass acts to lean the body backward relative to its center-of-mass. Since VAS has been shown to contribute to forward angular momentum in early stance (Neptune and McGowan, 2011), we expected that the BL condition would also require increased VAS output. To test these expectations, we performed additional analyses to determine the contribution of intact VAS to body support (i.e., vertical acceleration of the body center-of-mass) and sagittal plane angular momentum in all three loading conditions using previously described methods (Zajac and Gordon, 1989; Neptune and McGowan, 2011). We identified muscle contributions to sagittal plane angular momentum by calculating muscle contributions to the time rate of change of angular momentum (i.e., external moment) as:

$$\dot{\vec{H}} = \vec{M} = \vec{r} \times \vec{F}_{GRF} \quad (1)$$

where \bar{r} is the moment arm vector from the foot center-of-pressure on the foot to the body's center-of-mass and \bar{F}_{GRF} is the vector of the muscle's contribution to the ground reaction force.

The results showed that during BL the intact VAS muscle activity was increased and the contributions to body support and forward angular momentum were considerably higher relative to FL and NL (Figure 6). Thus, the reduced FL intact knee joint loading compared to BL was likely due to a reduced demand placed on the intact leg VAS to provide body support and forward angular momentum.

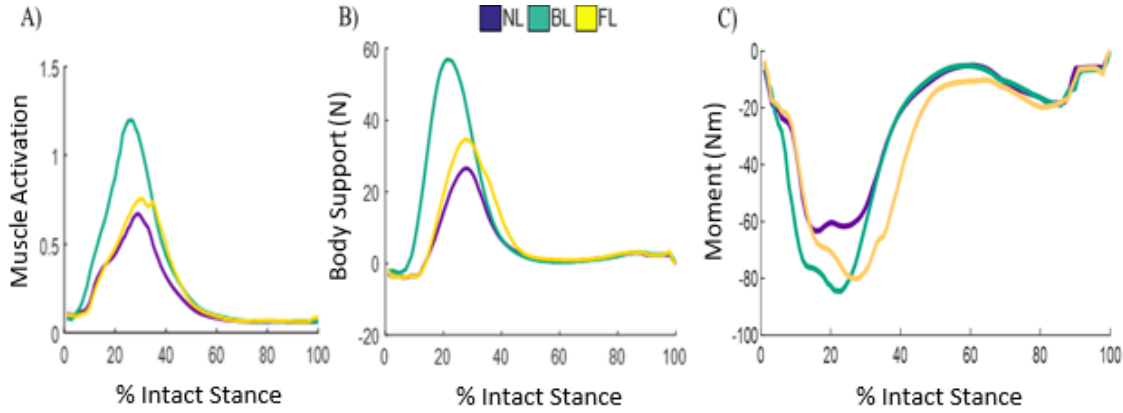


Figure 6: A) Intact VAS muscle activity, B) mean intact VAS contribution to body support over the stance phase for each of the three loading conditions using the SOC foot, C) Mean intact leg VAS contributions to sagittal plane external moment about the center-of-mass of the body during the three loading conditions using the SOC foot. Negative values indicate that the muscle is generating forward angular momentum.

METABOLIC COST

Our results are consistent with previous studies showing that metabolic cost increases during loaded walking relative to unloaded (Fallowfield et al., 2012; Schnall et al., 2012). GAS and SOL in particular showed markedly increased metabolic cost during BL and FL relative to NL (Figure 4). This is consistent with previous studies showing GAS and SOL exhibit increased muscle activity during loaded walking relative to unloaded (McGowan et al., 2008; Silder et al., 2013) and are the primary muscles that respond to increased demand for body support and forward propulsion with increased loads (McGowan et al., 2009). Additional muscles that are responsible for body support, such as the intact and residual GMED (McGowan et al., 2009), also showed increased metabolic cost in both BL and FL (Figures 4 and 5).

While FL resulted in lower knee joint loads relative to BL (Figures 1 and 2), we found that BL consistently produced lower metabolic cost relative to FL (Figure 3). The primary contributor to the increased metabolic cost during FL was the intact HAM (Figure 4). During FL, the added anterior mass acts to lean the body forward relative to its center-of-mass. Since HAM has been shown to be key contributor to generating backward angular momentum in early stance (Neptune and McGowan, 2011), we expected that the FL condition would require increased output from HAM. An analysis of HAM contributions to sagittal plane angular momentum showed that increased HAM output was indeed required to control sagittal plane angular momentum during FL relative to both NL and BL (Figure 7), which ultimately contributed to the increased metabolic cost of FL.

Previous studies have shown that increased HAM output reduces VAS contributions to body support (Fey et al., 2012) and that HAM contributions to knee joint compression forces are reduced relative to VAS during walking (Sasaki and Neptune, 2010). Thus, increased HAM output during FL may also be a compensation strategy to offload the intact knee joint loads.

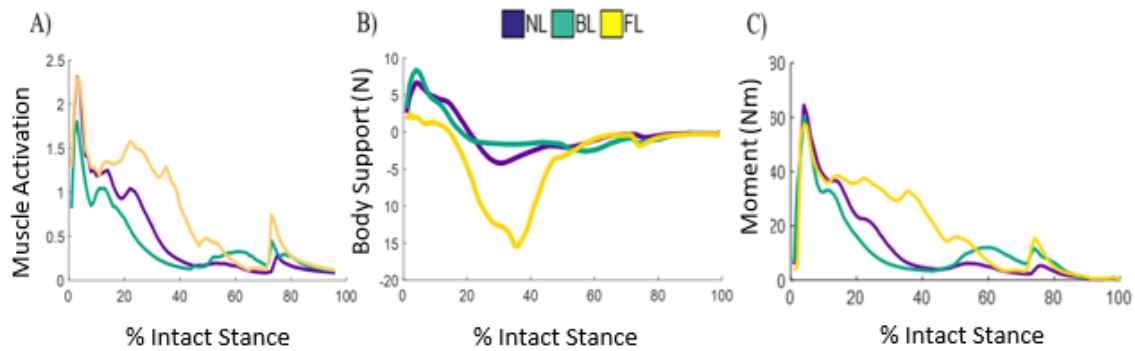


Figure 7: A) Intact HAM muscle activity, B) mean intact HAM contribution to body support over the stance phase for each of the three loading conditions using the SOC foot, C) Mean intact leg HAM contributions to sagittal plane external moment about the center-of-mass of the body during the three loading conditions using the SOC foot. The moment was calculated by cross multiplying the distance between the foot center-of-pressure and body center-of-mass with HAM contributions to the ground reaction forces. Positive values indicate that the muscle is generating backward angular momentum.

Limitations and Future Work

The primary limitation of this study was that the results may not be generalizable to all lower limb prosthesis users as our study was based on analysis from one subject. While this subject was deemed representative because of his age (Mayfield et al., 2000), and height and weight (Fryar et al., 2018), many other factors influence amputee gait mechanics. For example, prosthesis fit and the type of interface between the socket and residual limb (such as vacuum suspension and pin-locking) influence user comfort, and thus a larger sample size would help validate the results of this study. We also focused on the influence of passive elastic energy-storage-and-return (ESAR) feet on metabolic cost and joint loading. An alternative commercially available option to ESAR feet are powered ankle-foot prostheses. Some studies suggest that powered feet can provide substantial benefit to the amputee population (Grabowski and D'Andrea, 2013; Herr and Grabowski, 2012; Esposito et al., 2016) while other studies suggest mixed results (Aldridge et al., 2012; Ferris et al., 2012; Gates et al., 2013; Esposito and Wilken, 2014). Prosthetic feet with damping properties might also provide benefit to amputees (Portnoy et al., 2012; De Asha et al., 2013; Johnson et al., 2014). Therefore, future work should investigate the ability of these devices to reduce metabolic cost and joint loading during various load carriage conditions. Future work should also be focused on not only anterior and posterior load carriage but also loads carried to the left or right of the body.

An additional aspect of load carriage walking performance that should be studied is dynamic balance. With the functional loss of the plantar flexors, amputees not only exhibit increased joint loading asymmetries and metabolic cost but also have a significantly

altered angular momentum profiles relative to non-amputees (Silverman and Neptune, 2011). The present study showed that the different load conditions required increased regulation of whole body angular momentum. Thus, future work should focus on how muscles work together in synergy to provide balance control in response to different loading conditions, which would provide evidence to assist clinicians in the prescription of prostheses for patients who are likely to carry various loads.

Chapter 5: Conclusion

In summary, the increased asymmetric knee loading during load carriage observed in this study suggests that amputees rely on their intact limb as a compensatory strategy to meet the increased demands of carrying a front or back load. Carrying a front load reduced intact knee joint loading in comparison to carrying a back load through a reduced demand placed on the intact leg VAS to provide body support. However, the increased demand placed on the intact HAM during front load carriage elevated the metabolic cost in comparison to back loads. This tradeoff between metabolic cost and knee joint loading while carrying a back load versus a front load should be taken into consideration when determining load carriage technique. The relatively minor influence of currently available ESAR feet highlights the need to improve prosthetic foot design to reduce metabolic cost and joint loading during load carriage.

Appendix

The following figures include data not included in the main thesis depicting individual muscle forces and muscle contributions to metabolic cost, body support, forward propulsion and sagittal plane balance control while wearing the four prosthesis in the three loading conditions.

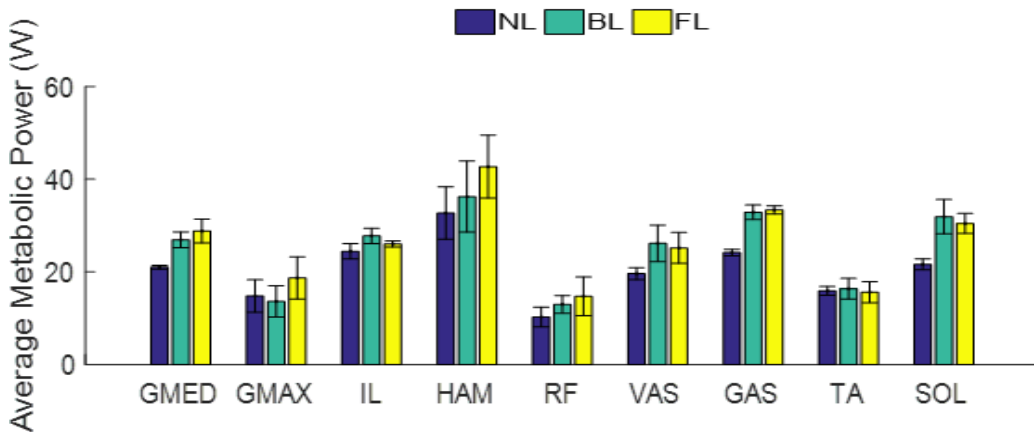


Figure A1: Mean \pm one standard deviation of total average metabolic power (W) of intact leg muscles throughout gait cycle while wearing the SF foot in the three loading conditions.

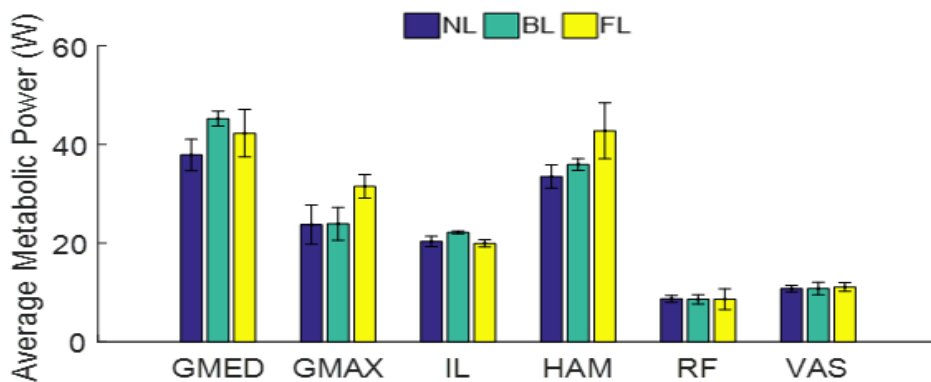


Figure A2: Mean \pm one standard deviation of total average metabolic power (W) of residual leg muscles throughout gait cycle while wearing the SF foot in the three loading conditions.

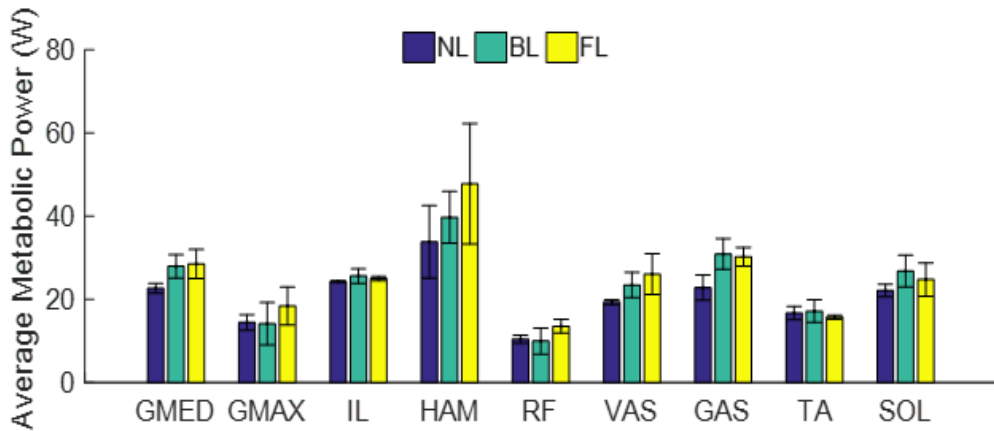


Figure A3: Mean \pm one standard deviation of total average metabolic power (W) of intact leg muscles throughout gait cycle while wearing the HW foot in the three loading conditions.

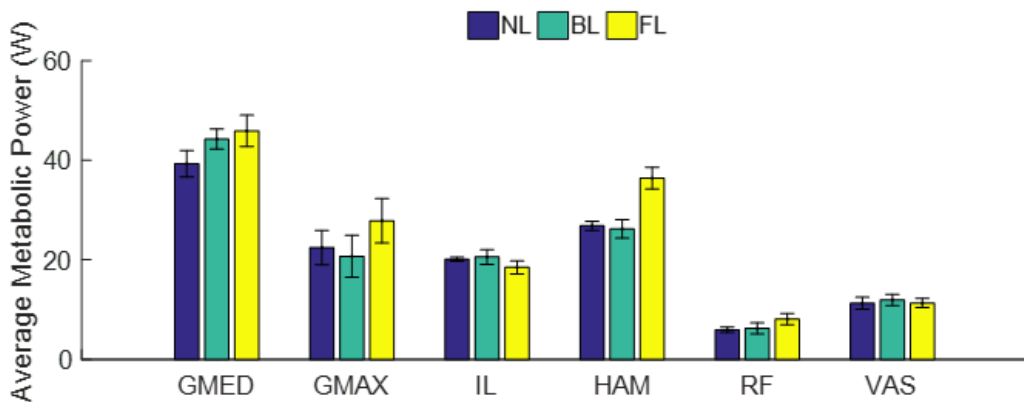


Figure A4: Mean \pm one standard deviation of total average metabolic power (W) of residual leg muscles throughout gait cycle while wearing the HW foot in the three loading conditions.

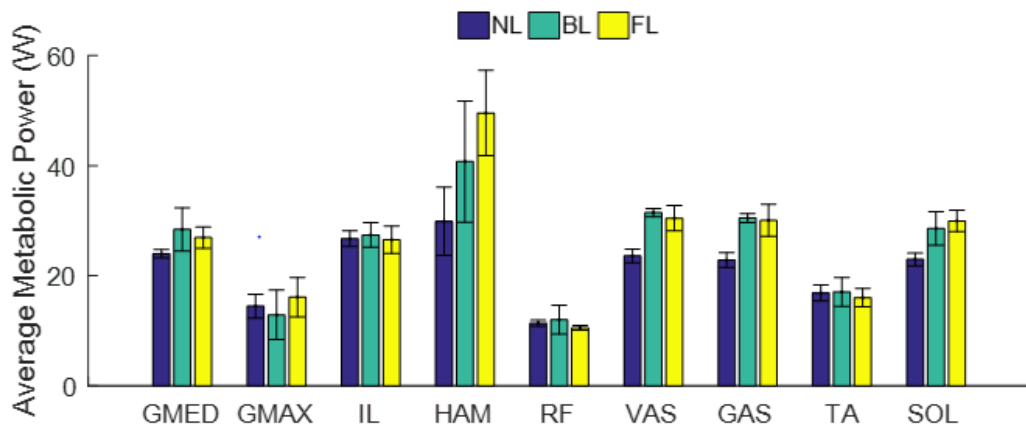


Figure A5: Mean \pm one standard deviation of total average metabolic power (W) of intact leg muscles throughout gait cycle while wearing the DK foot in the three loading conditions.

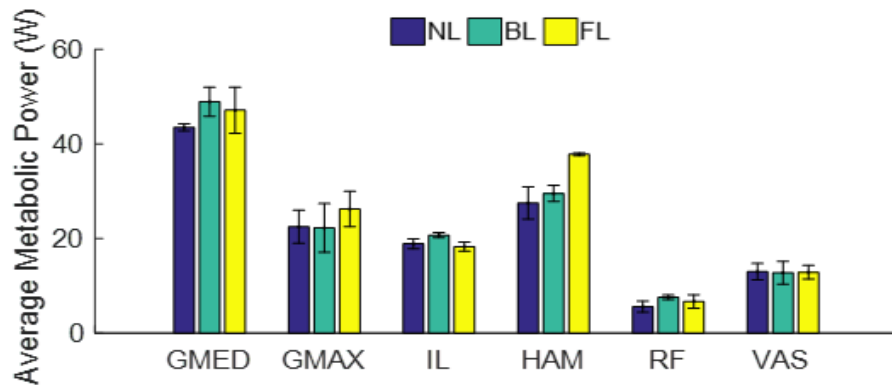


Figure A6: Mean \pm one standard deviation of total average metabolic power (W) of residual leg muscles throughout gait cycle while wearing the DK foot in the three loading conditions.

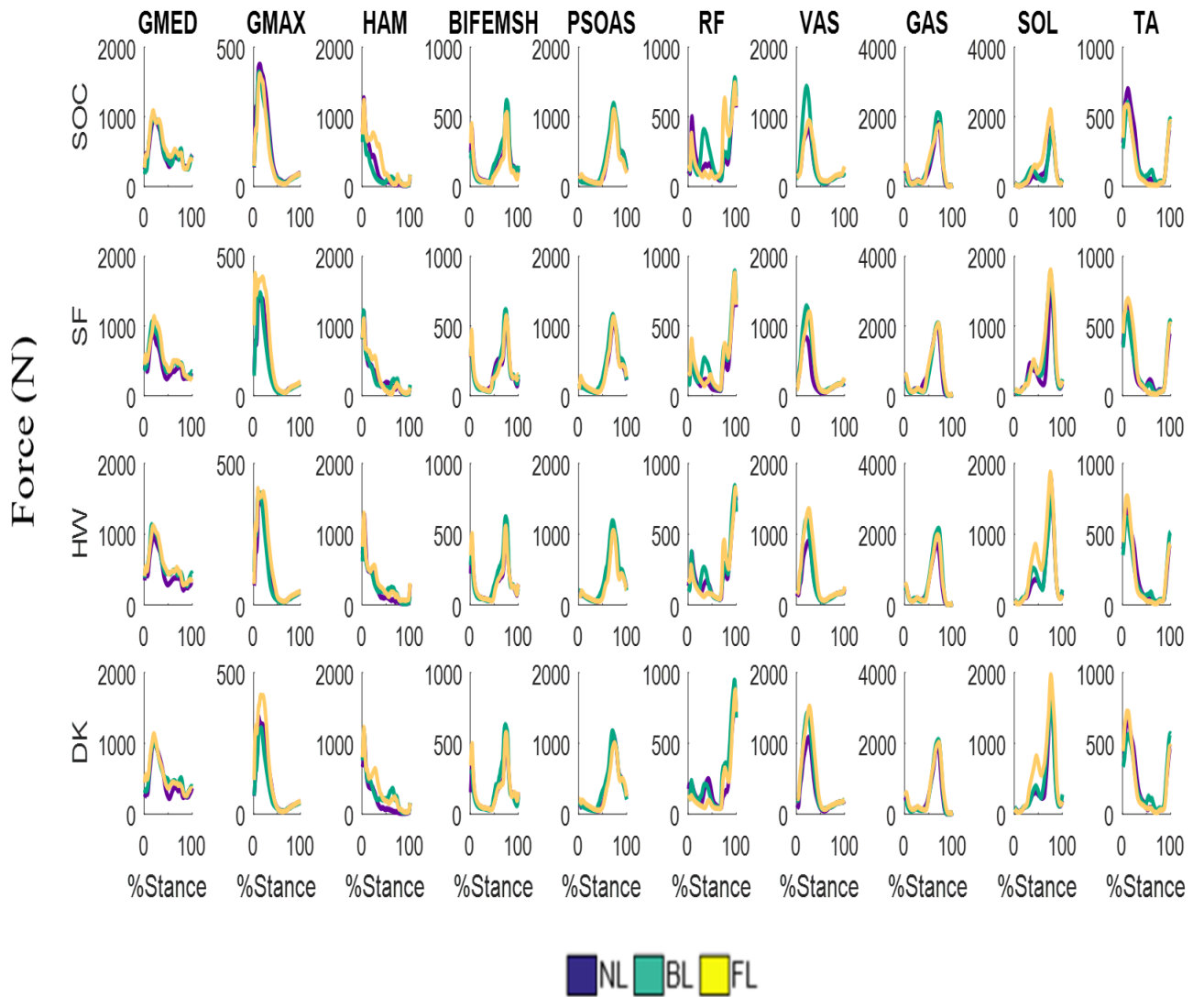


Figure A7: Mean intact muscle forces while wearing the four study prostheses across the three loading conditions.

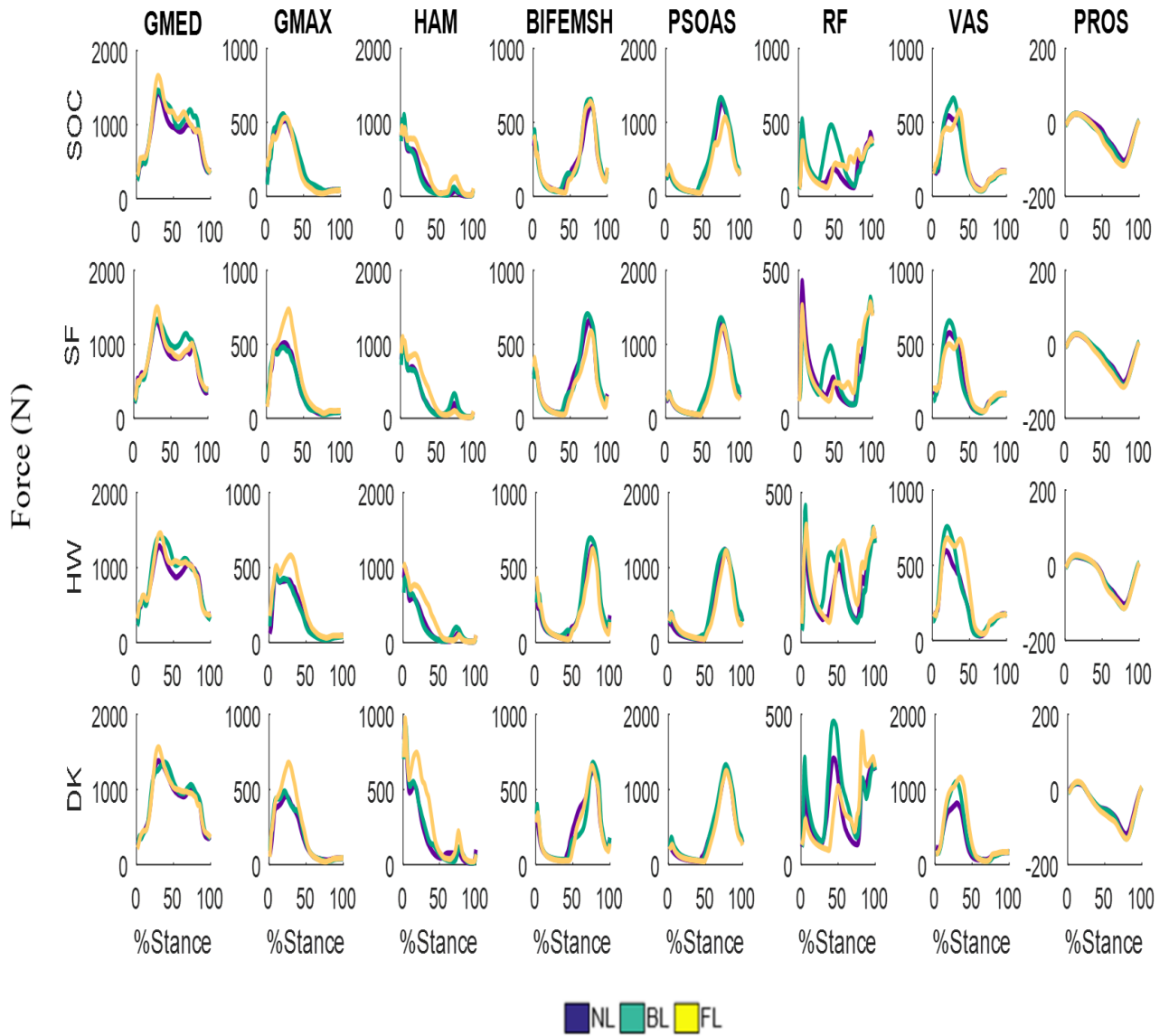


Figure A8: Mean residual muscle forces while wearing the four study prostheses across the three loading conditions.

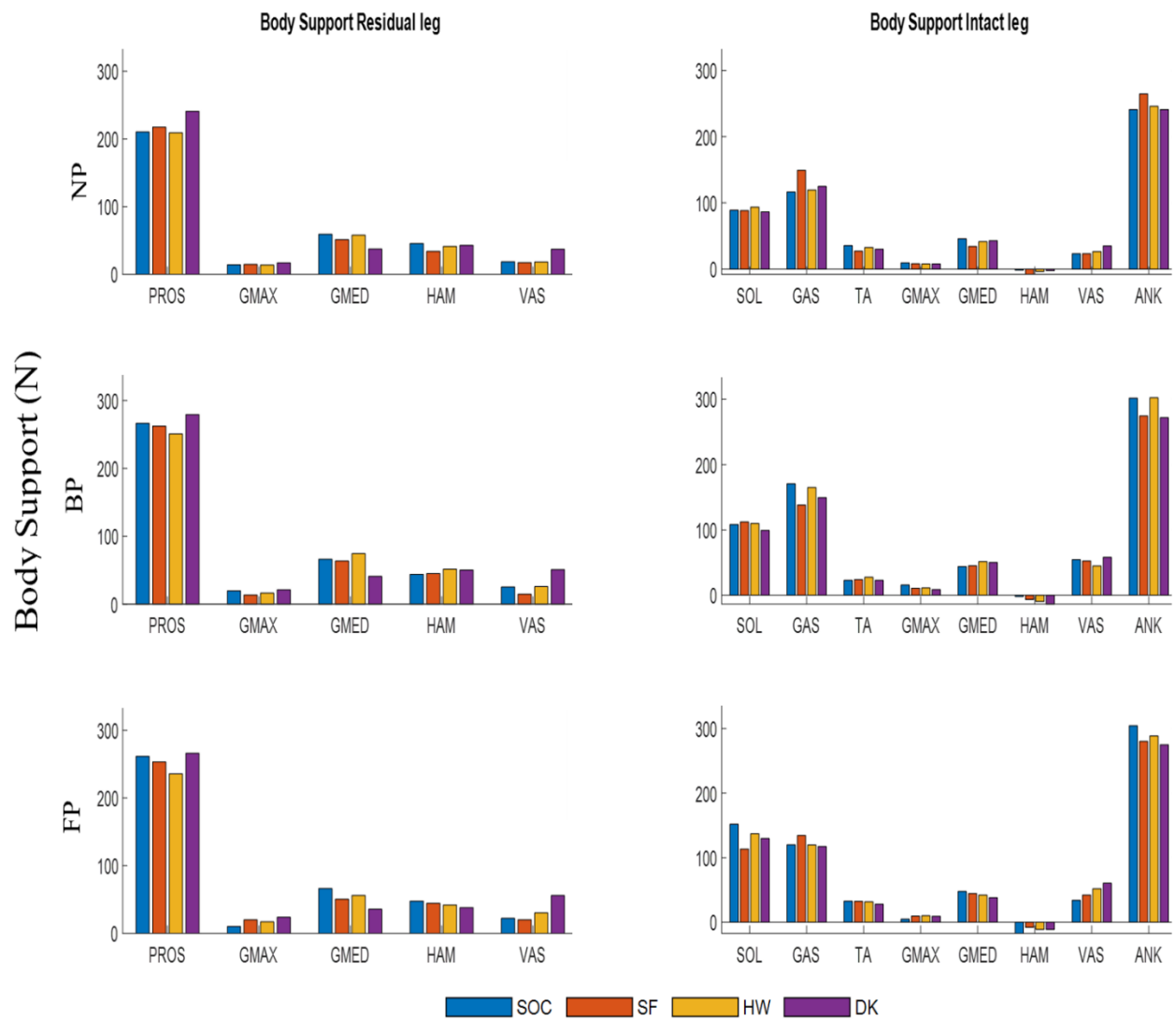


Figure A9: Mean intact and residual muscle contributions to body support impulses while wearing the four study prostheses across the three loading conditions.

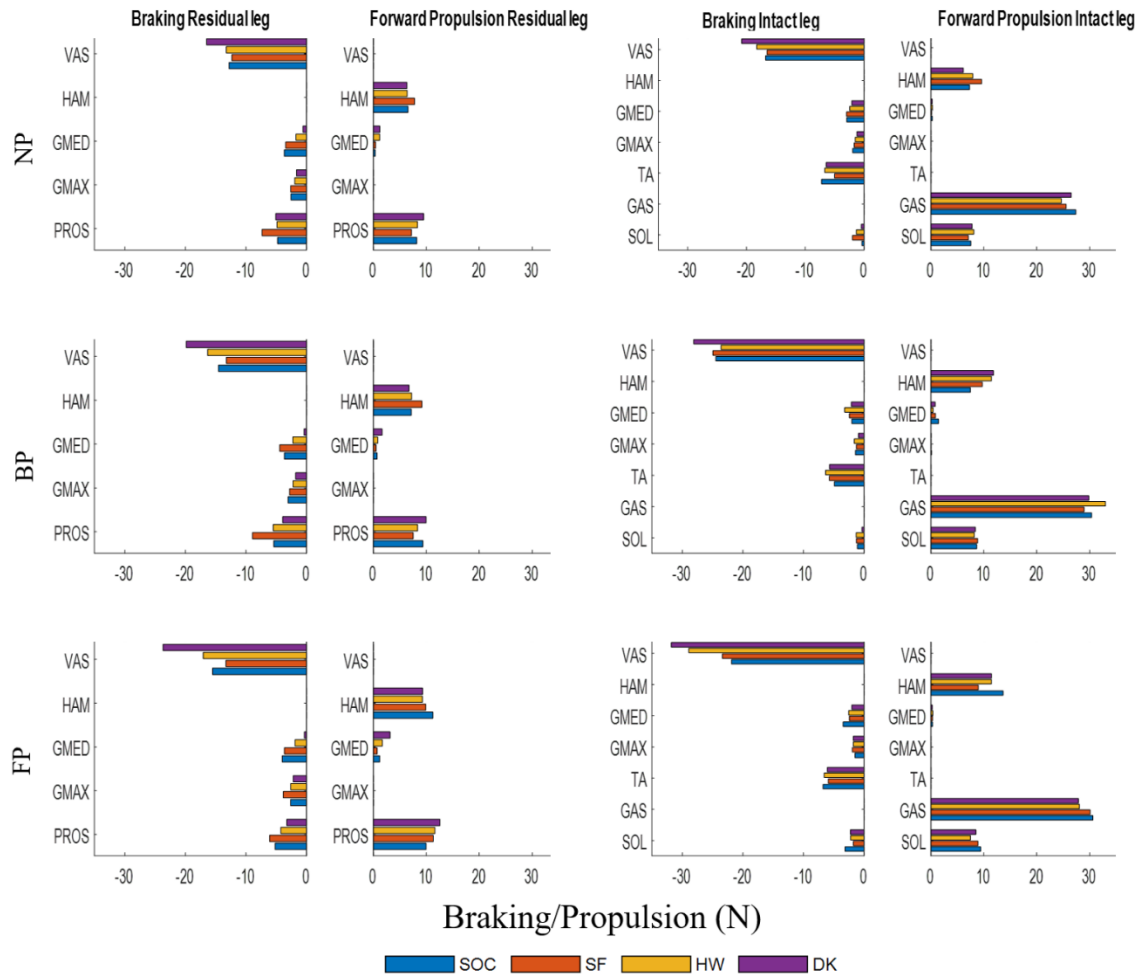


Figure A10: Mean intact and residual muscle contributions to braking and forward propulsion impulses while wearing the four study prostheses across the three loading conditions.

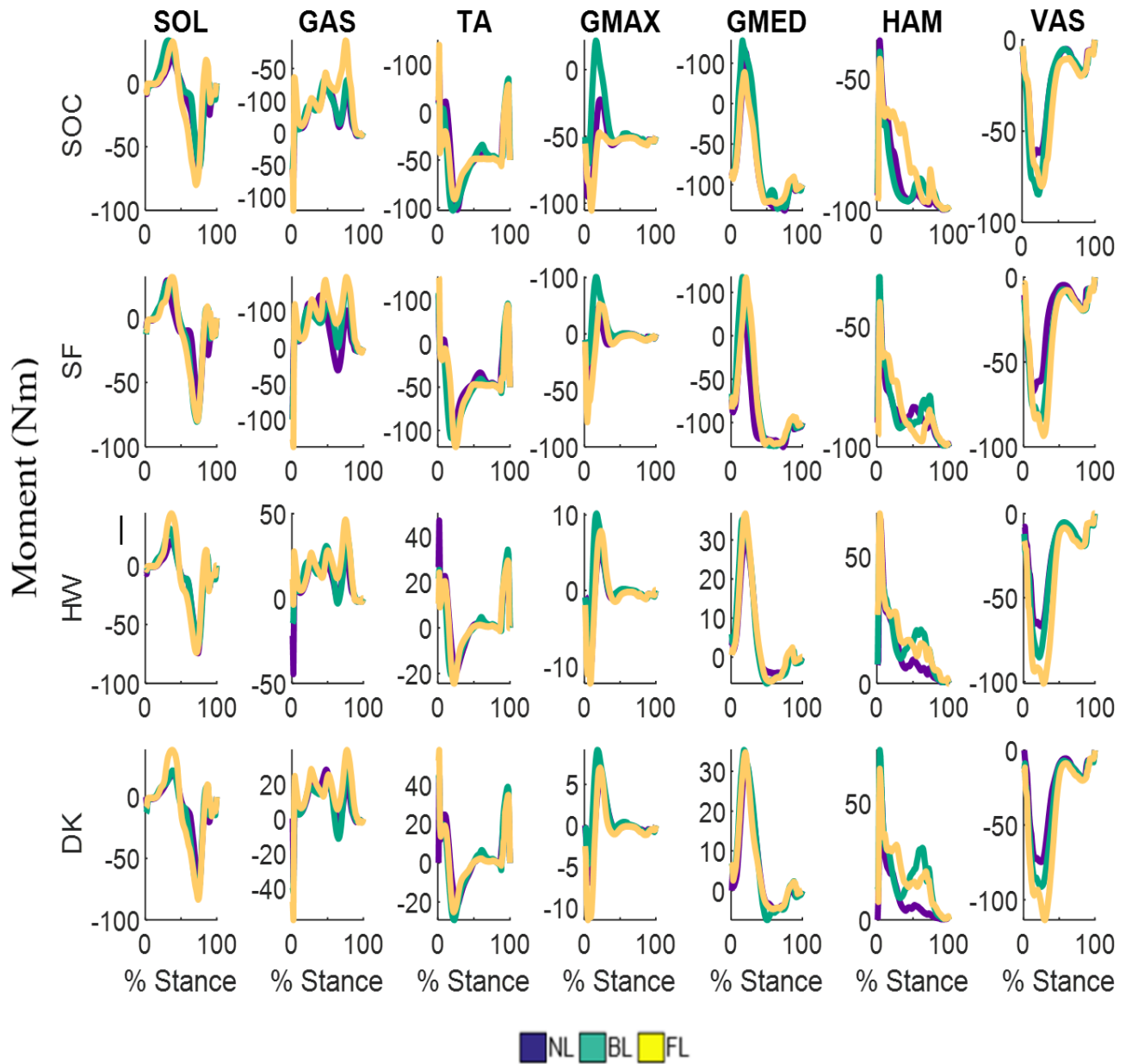


Figure A11: Mean intact leg muscle contributions to sagittal plane external moment about the center-of-mass of the body while wearing the four study prostheses across the three loading conditions.

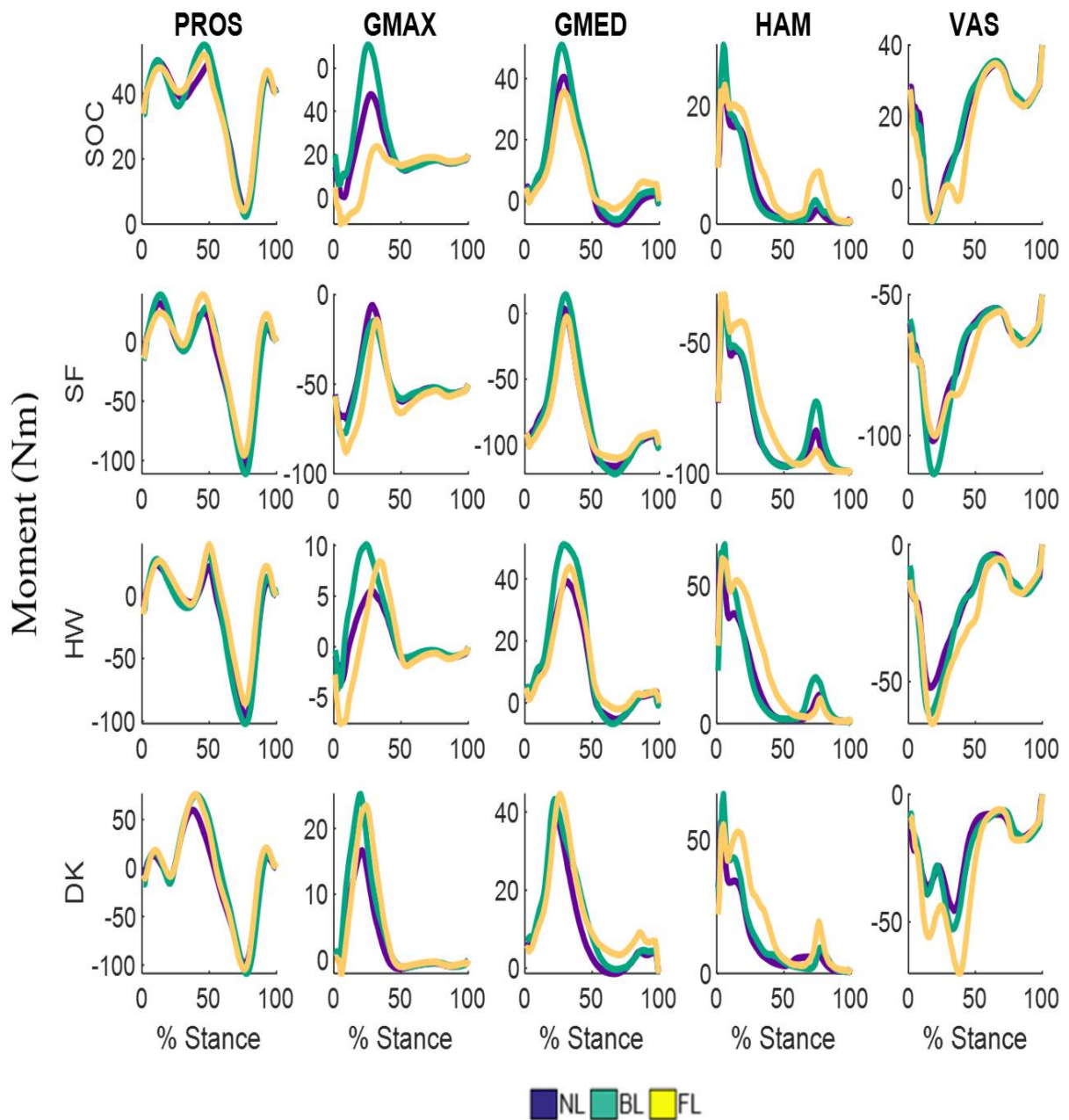


Figure A12: Mean residual leg muscle contributions to sagittal plane external moment about the center-of-mass of the body while wearing the four study prostheses across the three loading conditions.

References

- Aldridge, J. M., Sturdy, J. T., & Wilken, J. M. (2012). Stair ascent kinematics and kinetics with a powered lower leg system following transtibial amputation. *Gait & Posture*, 36(2), 291–295.
- Anderson, F. C., & Pandy, M. G. (2003). Individual muscle contributions to support in normal walking. *Gait & Posture*, 17(2), 159–169.
- Burke, M. J., Roman, V., & Wright, V. (1978). Bone and joint changes in lower limb amputees. *Annals of the Rheumatic Diseases*, 37, 252–254.
- Cappozzo, A., Cappello, A., Croce, U. D., & Pensalfini, F. (1997). Surface-marker cluster design criteria for 3-D bone movement reconstruction. *IEEE Transactions on Biomedical Engineering*, 44(12), 1165–1174.
- De Asha, A. R., Munjal, R., Kulkarni, J., & Buckley, J. G. (2013). Walking speed related joint kinetic alterations in trans-tibial amputees: impact of hydraulic “ankle” damping. *Journal of Neuroengineering and Rehabilitation*, 10, 107.
- Delp, S. L., Anderson, F. C., Arnold, A. S., Loan, P., Habib, A., John, C. T., ... Thelen, D. G. (2007). OpenSim: Open-Source Software to Create and Analyze Dynamic Simulations of Movement. *IEEE Transactions on Biomedical Engineering*, 54(11), 1940–1950.
- Dembia, C. L., Silder, A., Uchida, T. K., Hicks, J. L., & Delp, S. L. (2017). Simulating ideal assistive devices to reduce the metabolic cost of walking with heavy loads. *PloS One*, 12(7), e0180320.
- Doyle, S. S., Lemaire, E. D., Besemann, M., & Dudek, N. L. (2014). Changes to level ground transtibial amputee gait with a weighted backpack. *Clinical Biomechanics*, 29(2), 149–154.
- Doyle, S. S., Lemaire, E. D., Besemann, M., & Dudek, N. L. (2015). Changes to transtibial amputee gait with a weighted backpack on multiple surfaces. *Clinical Biomechanics*, 30(10), 1119–1124.
- Fallowfield, J. L., Blacker, S. D., Willems, M. E. T., Davey, T., & Layden, J. (2012). Neuromuscular and cardiovascular responses of Royal Marine recruits to load carriage in the field. *Applied Ergonomics*, 43(6), 1131–1137.
- Ferris, A. E., Aldridge, J. M., Rábago, C. A., & Wilken, J. M. (2012). Evaluation of a Powered Ankle-Foot Prosthetic System During Walking. *Archives of Physical Medicine and Rehabilitation*, 93(11), 1911–1918.

- Fey, N. P., Klute, G. K., & Neptune, R. R. (2011). The influence of energy storage and return foot stiffness on walking mechanics and muscle activity in below-knee amputees. *Clinical Biomechanics*, 26(10), 1025–1032.
- Fey, N. P., Klute, G. K., & Neptune, R. R. (2012). Optimization of Prosthetic Foot Stiffness to Reduce Metabolic Cost and Intact Knee Loading During Below-Knee Amputee Walking: A Theoretical Study. *ASME Journal of Biomechanical Engineering*, 134(11): 111005(1-10).
- Fryar, C. D., Kruszon-Moran, D., Gu, Q., & Ogden, C. L. (2018). Mean Body Weight, Height, Waist Circumference, and Body Mass Index Among Adults: United States, 1999–2000 Through 2015–2016. *National Health Statistics Reports*, Number 122.
- Gates, D. H., Aldridge, J. M., & Wilken, J. M. (2013). Kinematic comparison of walking on uneven ground using powered and unpowered prostheses. *Clinical Biomechanics*, 28(4), 467–472.
- Grabowski, A. M., & D’Andrea, S. (2013). Effects of a powered ankle-foot prosthesis on kinetic loading of the unaffected leg during level-ground walking. *Journal of NeuroEngineering and Rehabilitation*, 10(1), 49.
- Herr, H. M., & Grabowski, A. M. (2012). Bionic ankle-foot prosthesis normalizes walking gait for persons with leg amputation. *Proceedings of the Royal Society B: Biological Sciences*, 279(1728), 457–464.
- Johnson, L., De Asha, A. R., Munjal, R., Kulkarni, J., & Buckley, J. G. (2014). Toe clearance when walking in people with unilateral transtibial amputation: Effects of passive hydraulic ankle. *Journal of Rehabilitation Research and Development*, 51(3), 429–438.
- Klodd, E., Hansen, A., Fatone, S., & Edwards, M. (2010). Effects of prosthetic foot forefoot flexibility on gait of unilateral transtibial prosthesis users. *Journal of Rehabilitation Research & Development*, 47(9), 899–910.
- LaPrè, A. K., Price, M. A., Wedge, R. D., Umberger, B. R., & Sup, F. C. (2018). Approach for gait analysis in persons with limb loss including residuum and prosthesis socket dynamics. *International Journal for Numerical Methods in Biomedical Engineering*, 34(4), e2936.
- Mayfield, J. A., Reiber, G. E., Maynard, C., Czerniecki, J. M., Caps, M. T., & Sangeorzan, B. J. (2000). Trends in lower limb amputation in the Veterans Health Administration, 1989 - 1998. *Journal of Rehabilitation Research and Development* (Vol. 37).

- McGowan, C. P., Kram, R., & Neptune, R. R. (2009). Modulation of leg muscle function in response to altered demand for body support and forward propulsion during walking. *Journal of Biomechanics*, 42(7), 850–856.
- McGowan, C. P., Neptune, R. R., & Kram, R. (2008). Independent effects of weight and mass on plantar flexor activity during walking: implications for their contributions to body support and forward propulsion. *Journal of Applied Physiology (Bethesda, Md. : 1985)*, 105(2), 486–494.
- Neptune, R. R., & McGowan, C. P. (2011). Muscle contributions to whole-body sagittal plane angular momentum during walking. *Journal of Biomechanics*, 44(1), 6–12.
- Norvell, D. C., Czerniecki, J. M., Reiber, G. E., Maynard, C., Pecoraro, J. A., & Weiss, N. S. (2005). The prevalence of knee pain and symptomatic knee osteoarthritis among veteran traumatic amputees and nonamputees. *Archives of Physical Medicine and Rehabilitation*, 86(3), 487–493.
- Portnoy, S., Kristal, A., Gefen, A., & Siev-Ner, I. (2012). Outdoor dynamic subject-specific evaluation of internal stresses in the residual limb: Hydraulic energy-stored prosthetic foot compared to conventional energy-stored prosthetic feet. *Gait & Posture*, 35(1), 121–125.
- Riley, P. O., & Kerrigan, D. C. (1999). Kinetics of stiff-legged gait: induced acceleration analysis. *IEEE Transactions on Rehabilitation Engineering*, 7(4), 420–426.
- Russell Esposito, E., Aldridge Whitehead, J. M., & Wilken, J. M. (2016). Step-to-step transition work during level and inclined walking using passive and powered ankle–foot prostheses. *Prosthetics and Orthotics International*, 40(3), 311–319.
- Russell Esposito, E., & Wilken, J. M. (2014). Biomechanical risk factors for knee osteoarthritis when using passive and powered ankle–foot prostheses. *Clinical Biomechanics*, 29(10), 1186–1192.
- Sasaki, K., & Neptune, R. R. (2010). Individual muscle contributions to the axial knee joint contact force during normal walking. *Journal of Biomechanics*, 43(14), 2780–2784.
- Schnall, B. L., Hendershot, B. D., Bell, J. C., & Wolf, E. J. (2014). Kinematic analysis of males with transtibial amputation carrying military loads. *Journal of Rehabilitation Research and Development*, 51(10), 1505–1514.
- Schnall, B. L., Wolf, E. J., Bell, J. C., Gambel, J., & Bense, C. K. (2012). Metabolic analysis of male servicemembers with transtibial amputations carrying military loads. *The Journal of Rehabilitation Research and Development*, 49(4), 535.

- Shelburne, K. B., Torry, M. R., & Pandy, M. G. (2005). Muscle, ligament, and joint-contact forces at the knee during walking. *Medicine and Science in Sports and Exercise*, 37(11), 1948–1956.
- Silder, A., Delp, S. L., & Besier, T. (2013). Men and women adopt similar walking mechanics and muscle activation patterns during load carriage. *Journal of Biomechanics*, 46(14), 2522–2528.
- Silverman, A. K., & Neptune, R. R. (2011). Differences in whole-body angular momentum between below-knee amputees and non-amputees across walking speeds. *Journal of Biomechanics*, 44(3), 379–385.
- Silverman, A. K., & Neptune, R. R. (2012). Muscle and prosthesis contributions to amputee walking mechanics: A modeling study. *Journal of Biomechanics*, 45, 2271–2278.
- Silverman, A. K., & Neptune, R. R. (2014). Three-dimensional knee joint contact forces during walking in unilateral transtibial amputees. *Journal of Biomechanics*, 47, 2556–2562.
- Struyf, P. A., van Heugten, C. M., Hitters, M. W., & Smeets, R. J. (2009). The Prevalence of Osteoarthritis of the Intact Hip and Knee Among Traumatic Leg Amputees. *Archives of Physical Medicine and Rehabilitation*, 90(3), 440–446.
- Uchida, T. K., Hicks, J. L., Dembia, C. L., & Delp, S. L. (2016). Stretching Your Energetic Budget: How Tendon Compliance Affects the Metabolic Cost of Running. *PloS One*, 11(3), e0150378.
- Umberger, B. R. (2010). Stance and swing phase costs in human walking. *Journal of The Royal Society Interface*, 7(50), 1329–1340.
- Umberger, B. R., Gerritsen, K. G. M., & Martin, P. E. (2003). A Model of Human Muscle Energy Expenditure. *Computer Methods in Biomechanics and Biomedical Engineering*, 6(2), 99–111.
- Zajac, F. E. (1989). Muscle and tendon: properties, models, scaling, and application to biomechanics and motor control. *Critical Reviews in Biomedical Engineering*, 17(4), 359–411.
- Zajac, F. E., & Gordon, M. E. (1989). Determining muscle's force and action in multi-articular movement. *Exercise and Sport Sciences Reviews*, 17, 187–230.

Zmitrewicz, R. J., Neptune, R. R., & Sasaki, K. (2007). Mechanical energetic contributions from individual muscles and elastic prosthetic feet during symmetric unilateral transtibial amputee walking: A theoretical study. *Journal of Biomechanics*, 40(8), 1824–1831.

Vita

Tylan Templin was raised in Granbury, Texas and graduated from Trinity Valley High School in 2012. He attended the University of Texas at Austin and graduated with a Bachelor of Science degree in Chemical Engineering in 2017. While pursuing his undergraduate degree he played wide receiver on the University of Texas football team. After graduating, he worked as an assistant at Capital Prosthetics and Orthotics. Ty was accepted into graduate school at the University of Texas at Austin in the Mechanical Engineering Department and joined Dr. Richard Neptune's Neuromuscular Biomechanics Lab in August, 2017.

Permanent email address: ty.templin@gmail.com

This thesis was typed by the author.